ISSN 0020-1685, Inorganic Materials, 2017, Vol. 53, No. 7, pp. 685–689. © Pleiades Publishing, Ltd., 2017.
Original Russian Text © S.Z. Imamaliyeva, T.M. Gasanly, V.P. Zlomanov, M.B. Babanly, 2017, published in Neorganicheskie Materialy, 2017, Vol. 53, No. 7, pp. 701–705.

Phase Equilibria in the Tl_5Te_3–Tl_9BiTe_6–Tl_9TbTe_6 System

S. Z. Imamaliyeva[a], *, T. M. Gasanly[b], V. P. Zlomanov[c], and M. B. Babanly[a]

[a] *M. Nagiyev Institute of Catalysis and Inorganic Chemistry, Academy of Sciences of Azerbaijan, Javid ave 113, Baku, AZ1143, Azerbaijan*

[b] *Baku State University, Khalilov str. 23, Baku, AZ1143, Azerbaijan*

[c] *Moscow State University, Moscow, 119991 Russia*

**e-mail: _samira@mail.ru*

Received September 24, 2016; in final form, January 30, 2017

Abstract—Phase equilibria in the Tl_5Te_3–Tl_9BiTe_6–Tl_9TbTe_6 system have been studied using differential thermal analysis, X-ray diffraction, and microhardness measurements. We have mapped out a number of vertical sections, the 760-K isothermal section of its phase diagram, and projections of its liquidus and solidus surfaces. The composition dependences of lattice parameters and microhardness have been obtained. The system has been shown to contain a continuous series of solid solutions, which crystallize in a tetragonal structure (Tl_5Te_3 type, sp. gr. *I*4/*mcm*).

Keywords: thallium tellurides, terbium tellurides, thallium bismuth tellurides, phase equilibria, liquidus surface, solid solutions, crystal lattice

DOI: 10.1134/S0020168517070093

INTRODUCTION

Chalcogenides of heavy *p*-block elements have attracted researchers' attention as functional materials possessing interesting optical, photoelectric, thermoelectric, and other properties [1–3]. Some of them are topological insulators and are thought to be potentially attractive for use in spintronics and quantum computers [4, 5]. Rare-earth tellurides are widely used in the fabrication of electronic devices, such as microbatteries and highly efficient multilayer solar cells [6]. According to ab initio calculation results [7], $LaBiTe_3$ is a topological insulator and possesses thermoelectric properties [8].

The thallium telluride Tl_5Te_3 has thermoelectric properties and is the most suitable parent compound for engineering novel composition materials. This compound crystallizes in tetragonal symmetry (sp. gr. *I*4/*mcm*, a = 8.930 Å, c = 12.598 Å, Z = 4) [9] and, owing to some specific features of its crystal structure, has a number of ternary analogs with the general formulas $Tl_4A^{IV}Te_3$ (A^{IV} = Sn, Pb) and $Tl_9B^{V}Te_6$ (B^{V} = Sb, Bi) [10–12].

These compounds possess thermoelectric properties [13–16], and Tl_9BiTe_6 offers a record high thermoelectric performance (ZT = 1.2 at 500 K) [15]. Moreover, according to Arpino et al. [17] Tl_5Te_3 and $[Tl_4](Tl_{1-x}Sn_x)Te_3$ have surface topological states.

The existence of Tl_9LnTe_6-type compounds—new structural analogs of Tl_5Te_3—was first demonstrated by Imamalieva et al. [18] and Babanly et al. [19]. They identified the melting behavior of these compounds and determined their melting points and lattice parameters. Data on their physical properties demonstrate that these compounds possess thermoelectric and magnetic properties [20–22].

To obtain complex phases of variable composition with the Tl_5Te_3 structure, Babanly et al. [23] and Imamalieva et al. [24, 25] studied phase equilibria in systems of Tl_5Te_3 and its analogs and identified continuous series of substitutional solid solutions.

As a continuation of our previous studies of such systems, this work focuses on the phase equilibria in the Tl_5Te_3–Tl_9BiTe_6–Tl_9TbTe_6 system.

The constituent tellurides of this system have been the subject of extensive studies. The Tl_9BiTe_6 compound melts congruently at 830 K and has a broad homogeneity range [11]. Doert and Böttcher [26] investigated the crystal structure of this compound and refined its lattice parameters: a = 8.855 Å and c = 13.048 Å (Z = 2). The Tl_9TbTe_6 compound decomposes peritectically at 780 K and crystallizes in tetragonal symmetry with lattice parameters a = 8.871 Å and c = 12.973 Å (Z = 4) [27]. The constituent binary systems Tl_5Te_3–Tl_9BiTe_6 [11] and Tl_5Te_3–Tl_9TbTe_6 [28] of

Some properties of the constituent tellurides and solid solutions of the Tl_9TbTe_6–Tl_9BiTe_6 system

Phase	Thermal events during heating, K	Tetragonal lattice parameters, Å		H_μ, MPa
		a	*c*	
Tl_9TbTe_6	780, 1110	8.871(2)	12.973(5)	1000
$Tl_9Bi_{0.2}Tb_{0.8}Te_6$	783–803, 1046	8.868(3)	12.985(6)	1090
$Tl_9Bi_{0.4}Tb_{0.6}Te_6$	790–815	8.864(2)	13.001(5)	1070
$Tl_9Bi_{0.6}Tb_{0.4}Te_6$	800–822	8.861(2)	13.015(6)	1060
$Tl_9Bi_{0.8}Tb_{0.2}Te_6$	805–825	8.858(4)	13.031(7)	1030
Tl_9BiTe_6	830	8.855(3)	13.048(5)	980

The error of determination was 3–4 K in the temperatures of thermal events and 20 MPa in microhardness.

the ternary system under investigation contain continuous series of solid solutions with the Tl_5Te_3 structure.

EXPERIMENTAL

The congruently melting compounds Tl_5Te_3 (723 K) and Tl_9BiTe_6 (830 K) were synthesized by melting elemental thallium, tellurium, and bismuth at temperatures slightly (30–50 K) above their melting points in silica ampules pumped down to ~10^{-2} Pa, followed by slow cooling (furnace-cooling). Given that Tl_9TbTe_6 melts incongruently [27, 28], the as-prepared, inhomogeneous cast alloy was ground into powder, thoroughly mixed, and pressed into a disk, which was then annealed at 750 K for 1000 h. All of the synthesized compounds were identified by differential thermal analysis (DTA) and X-ray diffraction.

Alloys of the Tl_5Te_3–Tl_9BiTe_6–Tl_9TbTe_6 system were prepared by melting the presynthesized constituent tellurides under vacuum. Given that even prolonged (1000 h) homogenizing annealing of the as-cast alloys failed to ensure equilibration of the samples, by analogy with previous studies the as-cast alloys were ground into powder, thoroughly mixed, and pressed into disks, which were then fired at 700 K for ~800 h.

DTA heating curves were obtained in the range from room temperature to ~1400 K at a heating rate of 10 K/min using a Netzsch 404 F1 Pegasus differential scanning calorimeter system. The crystal structure of the constituent tellurides and intermediate alloys was

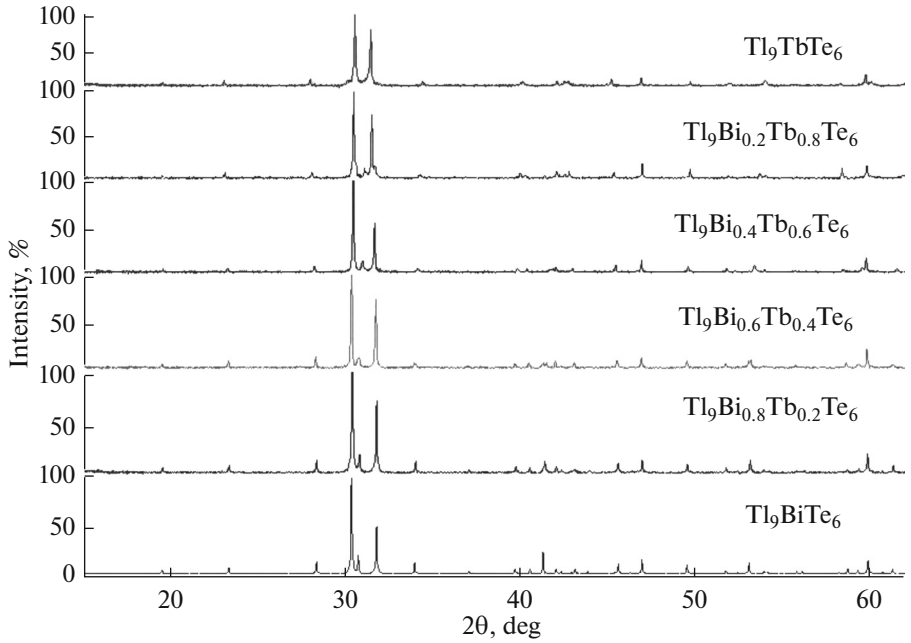

Fig. 1. X-ray powder diffraction patterns of alloys in the Tl_9TbTe_6–Tl_9BiTe_6 system.

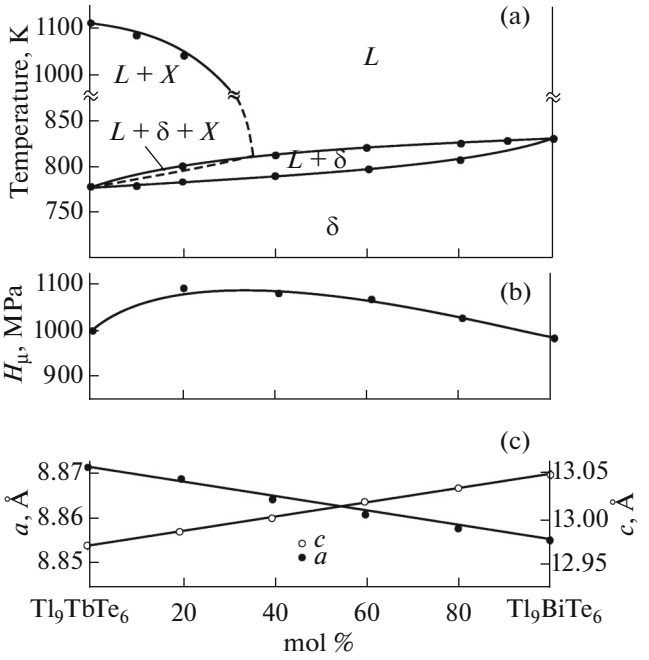

Fig. 2. Phase diagram (a) and composition dependences of microhardness (b) and lattice parameters (c) for alloys of the Tl_9TbTe_6–Tl_9BiTe_6 system.

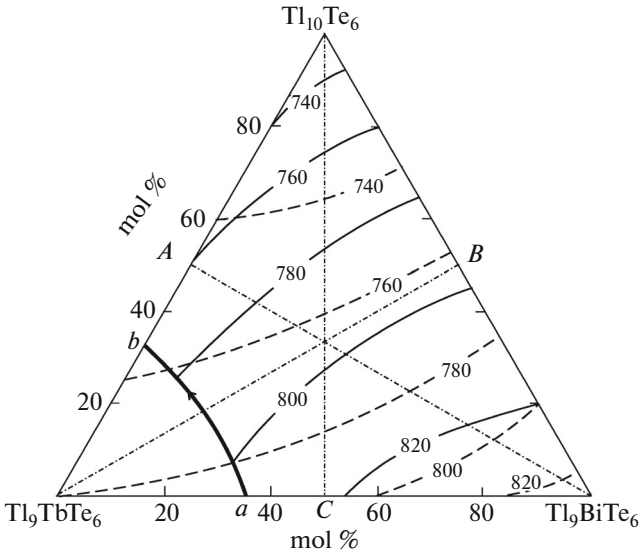

Fig. 3. Projections of the liquidus (solid lines) and solidus (dashed lines) surfaces in the Tl_5Te_3–Tl_9BiTe_6–Tl_9TbTe_6 system. The dot-dashed lines represent the cuts studied.

studied by X-ray diffraction at room temperature on a Bruker D8 powder diffractometer (CuK_α radiation) in the angular range $2\theta = 10°–70°$. Microhardness measurements were performed on a PMT-3 microhardness tester and an indenter load of 0.2 N.

RESULTS AND DISCUSSION

A joint analysis of experimental data obtained in this study by the above techniques and of previous results [11, 28] on the Tl_5Te_3–Tl_9BiTe_6 and Tl_5Te_3–Tl_9TbTe_6 systems allowed us to identify phase equilibria in the Tl_5Te_3–Tl_9BiTe_6–Tl_9TbTe_6 system (table, Figs. 1–5).

X-ray diffraction results indicate the formation of a continuous series of solid solutions in the constituent binary system Tl_9TbTe_6–Tl_9BiTe_6. As seen in Fig. 1, the X-ray diffraction patterns of the constituent tellurides and intermediate alloys in this system are similar to that of Tl_5Te_3, with a slight shift of their reflections. The composition dependences of the lattice parameters (calculated with the Topas V3.0 program) for the solid solutions (table) follow Vegard's law to within the present experimental uncertainty (Fig. 2c).

The *T*–*x* phase diagram of the Tl_9TbTe_6–Tl_9BiTe_6 system (Fig. 2a) demonstrates the formation of a continuous series of solid solutions with the Tl_5Te_3 structure (δ-phase). However, the system is not pseudobinary because of the incongruent melting of Tl_9TbTe_6. In a wide composition range (>35 mol % Tl_9BiTe_6), we observe the primary crystallization of another refractory phase, *X* (presumably $TlTbTe_2$), which leads to the formation of the $L + X$ and $L + X + \delta$ phase regions in the phase diagram. Because of its narrow temperature range, the $L + X + \delta$ phase region was not detected in our experiments and is marked by a dashed line.

The composition dependence of microhardness in Fig. 2b is consistent with the phase diagram: it has a flat maximum, which is characteristic of systems with a continuous series of substitutional solid solutions [29].

The projection of the *T*–*x*–*y* phase diagram onto the Gibbs composition triangle (Fig. 3) indicates that the liquidus surface comprises two phase fields, corresponding to the primary crystallization of the *X*-phase and δ-solid solution. These surfaces are separated by curve *ab*, which represents the $L + X \leftrightarrow \delta$ peritectic equilibrium. The solidus is formed by a single surface (dashed isotherms), corresponding to the onset of the melting of the δ-phase.

Figure 4 shows the Tl_9BiTe_6–*A*, Tl_9TbTe_6–*B*, and Tl_5Te_3–*C* vertical sections through the phase diagram of the Tl_5Te_3–Tl_9BiTe_6–Tl_9TbTe_6 system (where *A*, *B*, and *C* represent the 1 : 1 alloys in the constituent binary systems).

It is seen in Figs. 4a and 4c that only the δ-phase crystallizes from the melt over the entire composition range on the Tl_9BiTe_6–*A* and Tl_5Te_3–*C* joins.

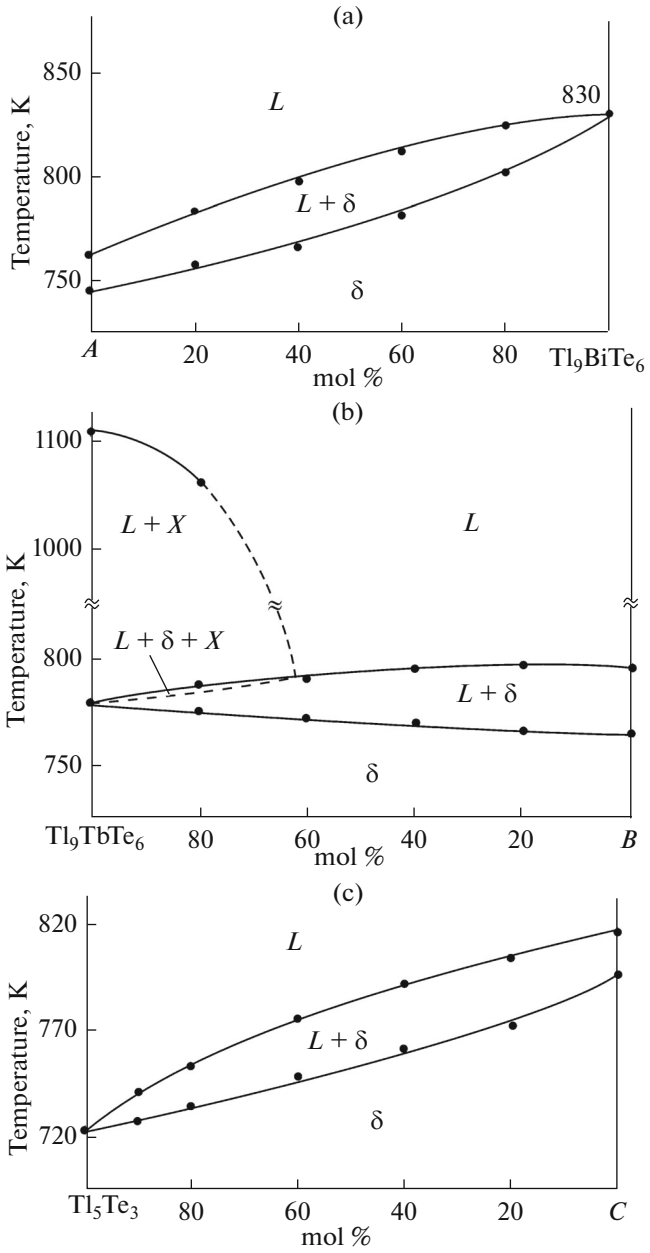

Fig. 4. (a) Tl_9BiTe_6–*A*, (b) Tl_9TbTe_6–*B*, and (c) Tl_5Te_3–*C* vertical sections through the phase diagram of the Tl_5Te_3–Tl_9BiTe_6–Tl_9TbTe_6 system.

On the Tl_9TbTe_6–*B* join (Fig. 4b), the δ-phase crystallizes from the melt in the composition range 0–60 mol % Tl_9TbTe_6. At higher Tl_9TbTe_6 contents, the first to crystallize is the *X*-phase. This is followed by the univariant peritectic reaction $L + X \leftrightarrow \delta$. As a result, the *X*-phase disappears and the excess melt crystallizes to give the δ-phase.

It is worth noting that, in the Tl_5Te_3–Tl_9BiTe_6–Tl_9TbTe_6 system, the directions of the tie lines in the $L + \delta$ two-phase regions do not coincide with the *T*–*x* planes of inner sections and vary with temperature. The directions of the tie lines at 760 K are clearly demonstrated by the corresponding isothermal section of the phase diagram (Fig. 5).

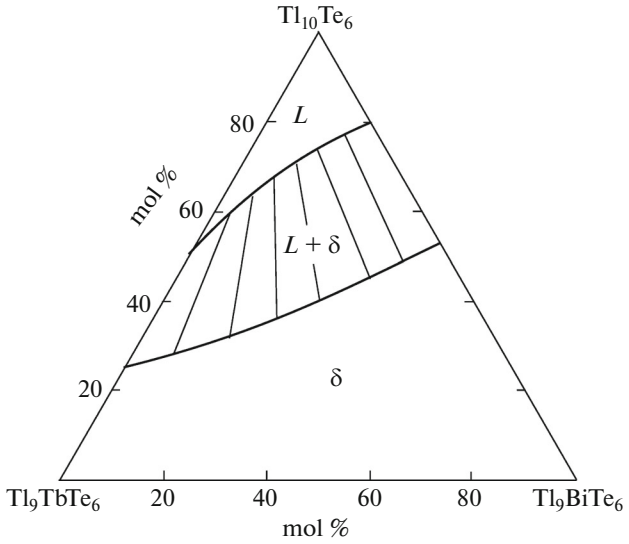

Fig. 5. 760-K isothermal section through the phase diagram of the Tl_5Te_3–Tl_9BiTe_6–Tl_9TbTe_6 system.

CONCLUSIONS

We have studied phase equilibria in the Tl_5Te_3–Tl_9BiTe_6–Tl_9TbTe_6 system. The system has been shown to contain a continuous series of solid solutions with a tetragonal structure (Tl_5Te_3 type, sp. gr. *I*4/*mcm*). The *T*–*x*–*y* phase diagram mapped out in this study and its isothermal sections can be useful in choosing melt compositions for the growth of single crystals of δ-solid solutions with tailored composition by directional solidification.

ACKNOWLEDGMENTS

This research was supported by the Science Foundation, State Oil Company of Azerbaijan Republic (Preparation and Characterization of Novel Functional Materials Based on Multicomponent Metal Chalcogenides for Alternative Energy Sources and Electronic Engineering Project, 2014).

REFERENCES

1. *Fiziko-khimicheskie svoistva poluprovodnikovykh veshchestv. Spravochnik* (Physicochemical Properties of Semiconducting Substances: A Handbook), Novoselova, A.V. and Lazarev, V.B., Eds., Moscow: Nauka, 1976.

2. Shevel'kov, A.V., Chemical aspects of thermoelectric materials engineering, *Usp. Khim.,* 2008, vol. 77, no. 1, pp. 3–21.

3. Zemskov, V.S., Shelimova, L.E., Karpinskii, O.G., Konstantinov, P.P., et al., Thermoelectric materials based on layered compounds in chalcogenide systems containing homologous series, *Termoelektr. Mezhdunarodn. Zh.,* 2010, no. 1, pp. 18–33.

4. Nechaev, I.A., Aguilera, I., De Renzi, V., Bona, A., Rizzini, A.L., et al., Quasiparticle spectrum and plasmonic excitations in the topological insulator Sb_2Te_3, *Phys. Rev. B: Condens. Matter Mater. Phys.,* 2015, vol. 91, paper 245 123.

5. Niesner, D., Otto, S., Hermann, V., Fauster, Th., et al., Bulk and surface electron dynamics in a *p*-type topological insulator $SnSb_2Te_4$, *Phys. Rev. B: Condens. Matter Mater. Phys.,* 2014, vol. 89, paper 081 404.

6. Jha, A.R., *Rare Earth Materials: Properties and Applications,* Boca Raton: CRC Press, 2014.

7. Yan, B., Zhang, H.-J., Liu, C.-X., Qi, X.-L., Frauenheim, T., and Zhang, S.-C., Theoretical prediction of topological insulator in ternary rare earth chalcogenides, *Phys. Rev. B: Condens. Matter Mater. Phys.,* 2010, vol. 82, paper 161 108(R).

8. Singh, N. and Schwingenschlogl, U., $LaBiTe_3$: an unusual thermoelectric material, *Phys. Status Solidi,* 2014, vol. 8, no. 9, pp. 805–808.

9. Schewe, I., Böttcher, P., and Schnering, H.G., The crystal structure of Tl_5Te_3 and its relationship to the Cr_5B_3, *Z. Kristallogr.,* 1989, vol. 188, pp. 287–298.

10. Babanly, M.B., Akhmad'yar, A., and Kuliev, A.A., Tl–Sb–Te system, *Zh. Neorg. Khim.,* 1985, vol. 30, no. 4, pp. 1051–1059.

11. Babanly, M.B., Akhmad'yar, A., and Kuliev, A.A., Tl_2Te–Bi_2Te_3–Te system, *Zh. Neorg. Khim.,* 1985, vol. 30, no. 9, pp. 2356–2359.

12. Gotuk, A.A., Babanly, M.B., and Kuliev, A.A., Phase equilibria in the Tl_2Te–SnTe and Tl_2Te–PbTe systems, *Uch. Zap. Azerb. Gos. Univ., Ser. Khim.,* 1978, no. 3, pp. 50–54.

13. Guo, Q., Chan, M., Kuropatwa, B.A., and Kleinke, H., Thermoelectric properties of Sn- and Pb-doped Tl_9BiTe_6 and Tl_9SbTe_6, *J. Appl. Phys.,* 2014, vol. 116, paper 183 702.

14. Kuropatwa, B.A., Guo, Q., Assoud, A., and Kleinke, H., Optimization of the telluride $Tl_{10-x-y}Sn_xBi_yTe_6$ for thermoelectric properties, *Z. Anorg. Allg. Chem.,* 2014, vol. 640, pp. 774–780.

15. Wolfing, B., Kloc, C., Teubner, J., and Bucher, E., High performance thermoelectric Tl_9BiTe_6 with an extremely low thermal conductivity, *Phys. Rev. Lett.,* 2001, vol. 36, no. 19, pp. 4350–4353.

16. Guo, Q., Chan, M., Kuropatwa, B.A., and Kleinke, H., Enhanced thermoelectric properties of variants of Tl_9SbTe_6 and Tl_9BiTe_6, *Chem. Mater.,* 2013, vol. 25, no. 20, pp. 4097–4104.

17. Arpino, K.E., Wallace, D.C., Nie, Y.F., Birol, T., et al., Evidence for topologically protected surface states and a superconducting phase in $[Tl_4](Tl_{1-x}Sn_x)Te_3$ using photoemission, specific heat, and magnetization measurements, and density functional theory, *Phys. Rev. Lett.,* 2014, vol. 112, paper 017 002.

18. Imamalieva, S.Z., Sadygov, F.M., and Babanly, M.B., New thallium neodymium tellurides, *Inorg. Mater.,* 2008, vol. 44, no. 9, pp. 935–938.

19. Babanly, M.B., Imamaliyeva, S.Z., Babanly, D.M., and Sadygov, F.M., Tl_9LnTe_6 (Ln = Ce, Sm, Gd) compounds—new structural analogs of Tl_5Te_3, *Azerb. Khim. Zh.,* 2009, no. 1, pp. 122–125.

20. Bangarigadu-Sanasy, S., Sankar, C.R., Schlender, P., and Kleinke, H., Thermoelectric properties of $Tl_{10-x}Ln_xTe_6$, with Ln = Ce, Pr, Nd, Sm, Gd, Dy, Ho and Er, and $0.25 < x < 1.32$, *J. Alloys Compd.,* 2013, vol. 549, pp. 126–134.

21. Bangarigadu-Sanasy, S., Sankar, C.R., Dube, P.A., Greedan, J.E., and Kleinke, H., Magnetic properties of Tl_9LnTe_6, Ln = Ce, Pr, Gd and Sm, *J. Alloys Compd.,* 2014, vol. 589, pp. 389–392.

22. Guo, Q. and Kleinke, H., Thermoelectric properties of hot-pressed Tl_9LnTe_6 (Ln = La, Ce, Pr, Nd, Sm, Gd, Tb) and $Tl_{10-x}La_xTe_6$ ($0.90 < x < 1.05$), *J. Alloys Compd.,* 2015, vol. 630, pp. 37–42.

23. Babanly, M.B., Tedenac, J.-C., Imamalieva, S.Z., Guseynov, F.N., and Dashdieva, G.B., Phase equilibria study in systems Tl–Pb(Nd)–Bi–Te new phases of variable composition on the base of Tl_9BiTe_6, *J. Alloys Compd.,* 2010, vol. 491, pp. 230–236.

24. Imamaliyeva, S.Z., Guseinov, F.N., and Babanly, M.B., Phase diagram of the Tl_5Te_3–Tl_4PbTe_3–Tl_9NdTe_6 system and some properties of solid solutions in it, *Khim. Probl.,* 2008, no. 4, pp. 640–646.

25. Imamaliyeva, S.Z., Guseinov, F.N., and Babanly, M.B., Phase equilibria and properties of solid solutions in the Tl_9NdTe_6–Tl_9BiTe_6–Tl_4PbTe_3 system, *Azerb. Khim. Zh.,* 2009, no. 1, pp. 49–53.

26. Doert, T. and Böttcher, P., Crystal structure of bismuth nonathallium hexatelluride $BiTl_9Te_6$, *Z. Kristallogr.,* 1994, vol. 209, pp. 95–100.

27. Imamaliyeva, S.Z., Gasanly, T.M., Sadygov, F.M., and Babanly, M.B., Phase diagram of the Tl_2Te–Tl_9TbTe_6 system, *Azerb. Chem. J.,* 2015, no. 3, pp. 93–97.

28. Imamalieva, S.Z., Gasanly, T.M., Zlomanov, V.P., and Babanly, M.B., Phase equilibria in the Tl_2Te–Tl_5Te_3–Tl_9TbTe_6 system, *Inorg. Mater,* 2017, vol. 53, no. 4, pp. 361–368.

29. Glazov, V.M. and Vigdorovich, V.N., *Mikrotverdost' metallov i poluprovodnikov* (Microhardness of Metals and Semiconductors), Moscow: Metallurgiya, 1969.

Translated by O. Tsarev